Atmos. Chem. Phys. Discuss., 12, 2783–2815, 2012
www.atmos-chem-phys-discuss.net/12/2783/2012/
doi:10.5194/acpd-12-2783-2012

Atmospheric Chemistry and Physics Discussions

Estimation of speciated and total mercury dry deposition at monitoring locations in Eastern and Central North America

L. Zhang[1], P. Blanchard[1], D. A. Gay[2], E. M. Prestbo[3], M. R. Risch[4], D. Johnson[5], J. Narayan[1], R. Zsolway[6], T. M. Holsen[7], E. K. Miller[8], M. S. Castro[9], J. A. Graydon[10], V. L. St. Louis[10], and J. Dalziel[11]

[1]Air Quality Research Division, Science and Technology Branch, Environment Canada, Toronto, ON, Canada
[2]Illinois State Water Survey, Prairie Research Inst., University of Illinois, Champaign, IL, USA
[3]Tekran Instruments Corporation, Toronto, ON, Canada
[4]US Geological Survey, Indianapolis, IN, USA
[5]Convex Logic, Gloucester, ON, Canada
[6]New Jersey Department of Environmental Protection, NJ, USA
[7]Department of Civil and Environmental Engineering, Clarkson University, Potsdam, NY, USA
[8]Ecosystems Research Group Ltd, Norwich, VT, USA
[9]University of Maryland Center for Environmental Science, Frostburg, MD, USA

[10] Department of Biological Sciences, University of Alberta, Edmonton, AB, Canada
[11] Air Quality Science Section, Environment Canada, Dartmouth, NS, Canada

Received: 16 January 2012 – Accepted: 17 January 2012 – Published: 27 January 2012

Correspondence to: L. Zhang (leiming.zhang@ec.gc.ca)

Published by Copernicus Publications on behalf of the European Geosciences Union.

ACPD
12, 2783–2815, 2012

Abstract

Dry deposition of speciated mercury, i.e., gaseous oxidized mercury (GOM), particulate bound mercury (PBM), and gaseous elemental mercury (GEM), was estimated for the year 2008–2009 at 19 monitoring locations in Eastern and Central North America. Dry deposition estimates were obtained by combining monitored 2–4 hourly speciated ambient concentration with modeled hourly dry deposition velocities (V_d) calculated using forecasted meteorology. Annual dry deposition of GOM + PBM was estimated to be in the range of 0.4 to 8.1 $\mu g\,m^{-2}$ at these locations with GOM deposition being mostly 5 to 10 times higher than PBM deposition, due to their different V_d values. Net annual GEM dry deposition was estimated to be in the range of 5 to 26 $\mu g\,m^{-2}$ at 18 sites and 33 $\mu g\,m^{-2}$ at one site. The estimated dry deposition agrees very well with limited surrogate-surface dry deposition measurements of GOM and PBM, and also agrees with litterfall mercury measurements conducted at multiple locations in Eastern and Central North America. This study suggests that GEM contributes much more than GOM + PBM to the total dry deposition at the majority of sites considered here; the only exception is at locations close to significant point sources where GEM and GOM + PBM contribute equally to the total dry deposition. The relative magnitude of the speciated dry deposition and their good comparison with litterfall deposition suggest that mercury in litterfall primarily originates from GEM, consistent with previous limited field studies. The study also supports previous analyses suggesting that total dry deposition of mercury is equally if not more important as wet deposition of mercury on a regional scale in Eastern North America.

1 Introduction

Atmospheric mercury (Hg) dry and wet deposition need to be quantified to reduce large gaps existing in global Hg mass balance estimates, assess Hg effects on various ecosystems, and attribute sources of deposited Hg for Hg emission controls (Mason

ACPD
12, 2783–2815, 2012

and Sheu, 2002; Mason et al., 2005; Lindberg et al., 2007; Selin et al., 2007). The Mercury Deposition Network (MDN) of the National Atmospheric Deposition Program (NADP) in the USA and Canada was established more than a decade ago to measure the wet deposition of Hg in precipitation (Vanarsdale et al., 2005; Prestbo and Gay, 2009; Risch et al., 2012b). More recently, the Atmospheric Mercury Network (AMNet) of NADP was also established to monitor speciated concentrations of atmospheric Hg for subsequent dry deposition estimation (NADP, 2011a–e). Mercury monitoring networks and/or monitoring sites also exist in many other parts of the world (Sakata and Asakura, 2008; Sprovieri et al., 2010). With the rich data set of speciated atmospheric Hg, modeling estimates of Hg dry deposition can be made.

Uncertainties in dry deposition estimates were believed to be larger than those in wet deposition estimates (Lindberg et al., 2007). Due to the constant cycling of Hg between different atmosphere-surface media as well as technological limitations, direct measurements of dry deposition are difficult and have large uncertainties (Schroeder et al., 1989; Bash et al., 2007; Gustin et al., 2008; Zhang et al., 2009). These large uncertainties hence led to the uncertainties of similar orders of magnitude in dry deposition models/parameterizations which were based on field measurements (Xu et al., 1999; Lyman et al., 2007; Marsik et al., 2007; Zhang et al., 2009; Bash et al., 2010). This further led to uncertainties in dry deposition estimates at monitoring locations and in Hg transport models. Our incomplete understanding of other physical and chemical processes involving Hg, and the different treatments of these processes in transport models further contributed to the uncertainties in Hg dry deposition estimates (Lin et al., 2006, 2007; Gbor et al; 2007; Bullock et al., 2008; Pongprueksa et al., 2008; Zhang et al., 2012).

Mercury wet deposition collected from MDN were discussed in many earlier studies (Vanarsdale et al., 2005; Prestbo and Gay, 2009; Risch et al., 2012b). This is not the case for measurement-based dry deposition estimates; particularly at regional scales, measurements are very limited (Miller et al., 2005; Engle et al., 2010). With the availability of speciated Hg concentrations data from AMNet, i.e., gaseous elemental Hg

ACPD
12, 2783–2815, 2012

(GEM), gaseous oxidized Hg (GOM) and particulate-bound Hg (PBM), it is now practical to provide more accurate estimation of Hg dry deposition for multiple locations. Furthermore, speciated Hg concentrations for dry deposition estimation is critical given substantial differences in dry deposition velocities and ambient concentrations among the different Hg species (Keeler and Dvonch, 2005; Zhang et al., 2009; Engle et al., 2010; Amos et al., 2012).

The purpose of this study is to provide more accurate model estimates of speciated and total Hg dry deposition for multiple locations across Eastern and Central North America. Dry deposition estimates for the years 2008 and 2009 at 19 monitoring locations were generated using AMNet concentrations. The estimated dry deposition was assessed using limited surrogate-surface dry deposition measurements (Castro et al., 2012; Huang et al., 2012) and substantial annual litterfall Hg measurements collected at multiple locations (Risch et al., 2012a). Total dry deposition and contributions from each individual Hg species are discussed in detail. Sources of Hg in litterfall and the relative importance of dry and wet deposition are also briefly discussed. The results are expected to provide useful information for the atmospheric Hg community as well as to the ecological research.

2 Methodology

2.1 Site information

Nineteen sites located in Central and Eastern USA and Canada are included in this study (Table 1, Fig. 1). Note that Rochester (NY43) and Rochester_B (NY95) were co-located but operated by two different research groups. All sites except ELA belong to AMNet. Population density, land use category (LUC), etc. are shown in Table S1 (Supplement, "SI"), leading to site categorization. Ten sites are identified as rural sites and the remainder are urban/suburban sites. Hg point source emissions within a 100 km circle of each site are also shown in Fig. 1. It should be noted that

ACPD
12, 2783–2815, 2012

point sources surrounding rural sites can be larger than those surrounding urban and suburban sites (e.g., Athens Super Site (OH02) and Piney Reservoir (MD08) versus nearby urban/suburban sites).

2.2 Air concentration measurements

Speciated Hg concentrations for the years 2008/2009 were used for this study. Available measurements are listed in Table 1. All data were collected using the Tekran Speciation systems (model 1130, 1135, and 2537; Tekran Inc., Toronto, Canada; Landis et al., 2002). Specific site conditions, operations, data quality control, data presentation can be found from individual studies, e.g., see Huang et al. (2010) for Rochester (NY95), Cheng et al. (2011) for ELA, and Mao and Talbot (2011) for Thompson Farm (NH06).

All sites except ELA have been quality assured by AMNet. The AMNet quality assurance program uses field operator procedures and software review of data to produce the final reported data. Individual hourly GEM and 2-hourly GOM and PBM averages are coded by the software as either valid or invalid observations and then the data has a final review by the network site liaison and the site operator. Only valid data is released for distribution and website download.

For field operations, initial data review is conducted by trained, onsite operators following standard operating procedures (SOP) for harmonized operation of all instruments. The SOPs include documentation and reporting of instrument maintenance and status on a weekly, monthly, quarterly and yearly basis. Additional procedures are in place to detect instrument problems using warning and action limits. An experienced site liaison is available for site consultation. Field operators regularly submit monthly site visit reports of instrument operation conditions, maintenance procedures completed and problems noted. These records are incorporated into the data record for final valid/invalid observations (see NADP, 2011a, b, c, d for specific steps).

Raw instrument data files are submitted regularly to the network for processing and quality assurance review. Hourly and 2-hourly averages are determined from the raw

ACPD
12, 2783–2815, 2012

observations using algorithms, with blank correction. The data is then subjected to an automated electronic quality assurance review procedure published in the Data Management Standard Operating Procedure document (NADP, 2011e). Examples of automated data flagging cover a multitude of performance checks include baseline stability, calibration response, contamination, sample volume and variability between dual sample cartridges, to name a few.

2.3 Dry deposition estimation

The inferential method, i.e., an atmospheric species' dry deposition flux (F) estimated as a product of its air concentration (C) and its dry deposition velocity (V_d), was employed in this study to estimate F for the three fractions of Hg (GEM, GOM and PBM). Fluxes for each fraction were calculated at the same time resolution as their concentrations. Considering that upward fluxes of GEM from re-emission of pre-deposited Hg and from natural emissions are frequently observed, net GEM dry deposition was used in the present study for constructing the dry deposition budget. Net GEM dry deposition was estimated as the difference between the calculated F and modeled total re-emission plus natural emission from the Global/Regional Atmospheric Heavy Metals Model (GRAHM) (Dastoor and Larocque, 2004; Dastoor et al., 2008), as discussed in Zhang et al. (2012).

V_d for GEM and GOM were calculated using the big-leaf dry deposition model described in Zhang et al. (2003):

$$V_d = \frac{1}{R_a + R_b + R_c}$$

where individual resistance terms include R_a as aerodynamic, R_b as quasi-laminar, and R_c as canopy resistance, respectively. R_c is parameterized as:

$$\frac{1}{R_c} = \frac{1 - W_{st}}{R_{st} + R_m} + \frac{1}{R_{ns}}$$

ACPD
12, 2783–2815, 2012

where W_{st} is the fraction of stomatal blocking under wet conditions, R_{st} is the stomatal resistance, calculated using a sunlit/shade stomatal resistance sub-model, R_m is the mesophyll resistance and is chosen as 500 s m^{-1} for GEM and 0 for GOM, and R_{ns} is the non-stomatal resistance which is a function of in-canopy, soil and cuticle resistance. Cuticle and soil resistance for GEM and GOM were scaled to those of SO_2 and O_3 using the following equation with two scaling parameters chosen as $\alpha = 0$ and $\beta = 0.1$ for GEM and $\alpha = 10$ and $\beta = 10$ for GOM:

$$\frac{1}{R_x(i)} = \frac{\alpha(i)}{R_x(SO_2)} + \frac{\beta(i)}{R_x(O_3)}$$

Note that the β value used here for GEM is smaller than the value (0.2) proposed in Zhang et al. (2009) to avoid overestimating V_d for GEM. This adjustment is based on GRAHM simulated GEM concentrations (Zhang et al., 2012). Parameters for GOM are the same as those for HNO_3, a common approach used in previous studies (Bullock et al., 2002; Miller et al., 2005; Marsik et al., 2007).

V_d for PBM was calculated using the size-segregated particle dry deposition model described in Zhang et al. (2001):

$$V_d = V_g + \frac{1}{R_a + R_s}$$

where V_g is the gravitational settling velocity, and R_s is the surface resistance parameterized as a function of collection efficiencies from Brownian diffusion, impaction and interception mechanisms. A log-normal size-distribution for PBM was assumed and V_d for each size bin was calculated and then aggregated into the bulk V_d based on the mass size distribution. A geometric mass mean diameter of 0.38 µm and a geometric standard deviation of 2.2 were used for the log-normal size distribution. This assumption is thought to be reasonable for inland sites where PBM is mainly associated with fine particles; however, V_d for coastal sites might be underestimated where PBM are frequently associated with coarse particles (Feddersen et al., 2012).

ACPD
12, 2783–2815, 2012

The original model of Zhang et al. (2001) used 15 LUCs, but here we used 26 LUCs, following Zhang et al. (2003; see further description in Table S1). Input parameters in Zhang et al. (2001) were given for each LUC and for five seasonal categories. This approach was discarded here; instead, the same approach developed in Zhang et al. (2003) was used. That is, for any input parameter (X) changing with season, a maximum (X_{max}) and a minimum value (X_{min}) were provided and were then interpolated to any day of the year based on the annual variation of leaf area index (LAI):

$$X(t) = X(\min) + \frac{\mathrm{LAI}(t) - \mathrm{LAI}(\min)}{\mathrm{LAI}(\max) - \mathrm{LAI}(\min)}[X(\max) - X(\min)]$$

where t represents any day of the year, and LAI(min) and LAI(max) represent minimum and maximum LAI values, respectively, during the year. Input parameters for the particle dry deposition model that need interpolation include a parameter for the characteristic radius of collectors, a parameter for calculating collection efficiency by Brownian diffusion, and a parameter for calculating collection efficiency by impaction (Zhang et al., 2001). Roughness for each LUC for the particle dry deposition model is the same as for the gaseous dry deposition model as described in Zhang et al. (2003).

Meteorological data used for driving the dry deposition models were from the archived data produced by the Canadian weather forecast model, an approach described in Brook et al. (1999). Meteorological variables representing the same time period as the Hg air concentration measurements for the surface and the first model-layer, typically at 40–50 m height, are available hourly at a horizontal grid resolution of 15 km by 15 km. Data for model grids containing the measurement sites were extracted from the archived data to calculate hourly V_d. Area-weighted land types within a 1 km radius of each site were used to calculate V_d (see Table 1 and Table S1).

2.4 Litterfall and wet deposition measurements

To assess the reasonableness of these dry deposition estimates, and explore the sources of Hg in litterfall, estimated speciated and total Hg dry deposition were

ACPD
12, 2783–2815, 2012

compared with collected litterfall mercury. The total net Hg dry deposition to a forest is the sum of Hg in litterfall, Hg captured by the canopy and then emitted back to the atmosphere, Hg washed off the canopy by precipitation (throughfall), and Hg deposited to underlying soils directly. Thus, litterfall deposition may be treated as the low-end estimation of total Hg dry deposition to a forest, if Hg emission from the underlying soil is limited. On the other hand, if soil Hg emissions are high and the ambient Hg concentrations above the forests are low, litterfall mercury might be higher than the dry deposition above the canopy due to the interception of emitted Hg by forest leaves. Based on the above arguments, it is reasonable to assume that total dry deposition and litetrfall deposition should be similar on regional scales, although the differences can be very large at individual sites. Thus, we compared the estimated dry deposition with measured litterfall deposition on regional-scale and at six collocated sites (see below for details). A better comparison would be to compare the estimated dry deposition with litterfall plus throughfall deposition, as was also done for ELA in this study.

Three-year average Hg litterfall measurements during 2007–2009 at 23 selected MDN sites, as described in detail by Risch et al. (2012a) were used for this study. The site information for litterfall measurements is listed in Table S2. Litterfall measurements were also made at the ELA (Graydon et al., 2008). Note that many AMNet sites are not collocated with MDN sites and thus are not at the same sites where the litterfall data were collected. Only six sites have both dry deposition estimation and litterfall measurements (Table 2).

Wet deposition collected by MDN during the years 2007–2009 were also used for the purpose of quantifying the relative importance of dry and wet deposition. A wet deposition map was created using three year average wet deposition of non-urban MDN monitoring sites. For this data, non-urban sites were defined as less than 400 people per square kilometer (km^2) within a 15-km radius of the site. The interpolated annual sums of Hg wet deposition were computed for an array of regularly spaced grid values using the sites that were within 300 km of each grid point. The boundary of the interpolated area was trimmed at the coast line and smoothed for values up

ACPD
12, 2783–2815, 2012

to 300 km from the outermost data points over land. Dry deposition of GOM + PBM, net dry deposition of GEM, and litterfall measurements were also marked on a wet deposition map for easy comparison.

3 Results and discussion

3.1 Air concentrations

Average annual concentrations during 2008–2009 ranged from 1.1 to 22.6 pg m^{-3} for GOM, 2.9 to 17.1 pg m^{-3} for PBM, and 1.2 to 2.1 ng m^{-3} for GEM (Fig. 2a, b) with geographical ratios of 20, 6, and 1.8, respectively. As expected, the species having shorter lifetime had the largest geographical variations. GOM only contributed 0.1–1.5 % to the total gaseous Hg (GOM+GEM) at these locations.

The highest annual concentrations for GEM were detected at several urban and sub-urban sites (e.g., 1.79 to 2.13 ng m^{-3} for NJ32, NJ54, NJ30 and UT97), whereas the lowest annual concentrations were detected in more remote rural areas (e.g., 1.24 to 1.37 ng m^{-3} for ELA, NH06, OK99 and NS01). The annual GEM concentration did not differ significantly between suburban and rural sites in the North-Eastern USA due to the many point and area sources in this region (Fig. S1) and the long atmospheric lifetime of GEM. The lowest annual concentrations of GOM and PBM were also detected at the same remote rural sites (ELA, NH06, OK99 and NS01) as with GEM; however, this was not the case for the highest concentrations of GOM and PBM. For example, UT97, MD08, WV99 and OH02 had the highest GOM concentrations and UT96, UT97, NJ54 had the highest PBM concentrations. Quite a few rural sites (e.g., WV99, OH02 and MD08) had GOM and PBM concentrations comparable to urban and suburban sites and similar for GEM.

Except at a few urban sites (NJ05, NJ30, NJ32 and UT97), GEM had higher concentrations in cold seasons (spring and winter) than in hot seasons (summer and fall) (Fig. S1 and Table S3). The seasonal patterns were likely caused by a combination

ACPD
12, 2783–2815, 2012

of reasons, including atmospheric chemistry, mixing layer height and dry deposition rate in different seasons. Seasonal variation of GOM and PBM were highly variable and also much larger than GEM. At many sites, GOM concentrations in spring were much higher than in any other season. At an urban site (UT97), GOM had a slightly higher concentration in summer and fall compared to winter and spring. At two other urban/suburban sites, GOM had concentrations that were a few times higher in summer compared to the fall and winter, but spring data at these two sites were not available. For PBM, the highest seasonal concentrations were observed in winter and the lowest were in the fall at the majority of the 19 sites. The same-season urban and rural pattern identified for GOM was not observed for PBM. The differences and similarities among the three Hg species in their geographical and seasonal patterns were caused by many factors include sources, transportation, chemical transformation and removal processes (Huang et al., 2010; Cheng et al., 2011; Mao and Talbot et al., 2011).

3.2 Dry deposition velocities

Based on dry deposition theory, if meteorological conditions are simialr, GOM and PBM should have larger V_d values over surfaces with larger roughness lengths (and thus higher friction velocities) than over smoother surfaces; and GEM should have larger V_d over canopies with larger LAI than over any other surface. For example, the estimated annual V_d of GOM over forest-dominated sites was in the range of 1.4–2.0 cm s^{-1}, and was close to 1.0 cm s^{-1} over urban areas (Fig. 2c). Values lower than 0.8 cm s^{-1} were also calculated for a few sites with small roughness length and/or weak wind speeds. In general, estimated V_d of PBM was 5–8 times smaller than V_d of GOM. Estimated annual V_d for GEM was mostly in the range of 0.05–0.08 cm s^{-1} over vegetated surfaces and below 0.05 cm s^{-1} over urban areas, and was generally 20–30 times smaller than those of GOM, and 2–6 times smaller than PBM. Calculated V_d values shown here are well within the range of published estimates (Zhang et al., 2009).

ACPD
12, 2783–2815, 2012

Estimated seasonal (or monthly) average V_d for GOM and PBM was higher during seasons with strong wind speed due to its strong dependence on turbulence intensity (friction velocity). As for GEM, V_d was higher during seasons with larger LAI. As an example, average diurnal and monthly V_d at the Kejimkujik site (NS01; a remote, more coastal site with forest coverage) are shown in Fig. S2. Wind was stronger in winter than in summer at this location and thus V_d of GOM and PBM was higher in winter. On the other hand, V_d of GEM was much higher in spring and summer than in winter due to the dominant effect of LAI. The relative changes (compared to their own annual average values) in the seasonal and diurnal V_d were also much larger for GEM (see normalized V_d, Fig. S2).

3.3 Estimated dry deposition fluxes

The estimated annual dry deposition of GOM + PBM ranged from 0.4 to 8.1 $\mu g\,m^{-2}\,yr^{-1}$ at the 19 sites. GOM contributed 0.3–7.8 $\mu g\,m^{-2}\,yr^{-1}$ to these fluxes, whereas PBM was relatively small, contributed only 0.1–0.8 $\mu g\,m^{-2}\,yr^{-1}$ (Fig. 3a). The estimated annual GEM dry deposition was in the range of 13 to 35 $\mu g\,m^{-2}\,yr^{-1}$ (Fig. 3b), much higher than originally assumed in many previous studies. Note that V_d values used for GEM are thought to be conservative, as discussed in Sect. 2. The very high dry deposition fluxes of GEM is certainly due to the 2–3 orders of magnitude higher concentration of GEM compared to those of GOM + PBM. As discussed in Zhang et al. (2012), GEM re-emission was around half of the GEM dry deposition on regional scales in Eastern North America, although the relative importance of re-emission/dry deposition varied significantly with locations. Using GRAHM modeled GEM re-emission and natural emission, net GEM dry deposition fluxes were estimated to be in the range of 4.8 to 23.3 $\mu g\,m^{-2}\,yr^{-1}$ for all the sites except for NS01, at 33 $\mu g\,m^{-2}\,yr^{-1}$ (Fig. 3b). The estimated net GEM dry deposition was still much higher than the estimated GOM + PBM dry deposition at the majority of the monitoring sites. It is noted that at several sites (MD08, UT07, WV99), net GEM dry deposition and dry deposition of GOM + PBM were in similar range of values (within a factor of 2).

ACPD
12, 2783–2815, 2012

Estimated dry deposition of GOM + PBM was generally higher at sites near significant Hg emissions, but not the case for estimated net GEM dry deposition. This is due to the strong dependence of GEM V_d on land types, meteorological conditions, and the small geographical variation of ambient GEM concentrations. For example, dry deposition of GOM + PBM was among the lowest at several rural/remote sites (ELA, Kejimkujik, Underhill), while net GEM dry deposition at these locations was among the highest. Thus, total dry deposition does not necessarily correlate with proximity to emission sources due to the dominance of GEM dry deposition.

These estimated annual GOM dry deposition amounts were in the same range as those in several previous studies based on measured ambient GOM concentrations. For example, Engle et al. (2010) and Lombard et al. (2011) obtained GOM dry deposition in the range of 0.5 to 5.3 $\mu g\,m^{-2}\,yr^{-1}$ at multiple locations in Central and Eastern USA; the only exception was for an urban site (Illinois) with estimated GOM deposition of 52 $\mu g\,m^{-2}\,yr^{-1}$, due to extremely high GOM concentrations. Here, estimated GOM dry deposition ranged from 0.3 to 4.5 $\mu g\,m^{-2}\,yr^{-1}$ for all the sites except for MD08, which was 7.8 $\mu g\,m^{-2}\,yr^{-1}$.

The estimated GOM + PBM dry deposition in the present study seems to be supported by limited field measurements using surrogate surfaces at several sites (MD08, NY20 and NY95). For example, Castro et al. (2012) obtained an annual dry deposition of 3.2 $\mu g\,m^{-2}\,yr^{-1}$ for GOM at MD08. However, the average GOM concentration during their study period (September 2009 to October 2010) was 9.1 $pg\,m^{-3}$. In comparison, the annual average GOM concentration for this study was 21.5 $pg\,m^{-3}$ and the estimated dry deposition was 7.8 $\mu g\,m^{-2}\,yr^{-1}$ (Figs. 2, 3). Model estimation agrees reasonably well with surrogate surface measurement at this site after concentration adjustment (e.g., < 10 % difference). Measured GOM + PBM dry deposition at NY20 during April 2009 to January 2010 was 0.8 $\mu g\,m^{-2}\,yr^{-1}$ and at NY95 during January to November 2009 was 4.4 $\mu g\,m^{-2}\,yr^{-1}$ (Huang et al., 2012). In comparison, the estimated dry deposition was 0.4 $\mu g\,m^{-2}\,yr^{-1}$ at NY20 during 2008 and is 3.9 $\mu g\,m^{-2}\,yr^{-1}$ at NY95 for September 2008 to December 2009. Good agreement between surrogate-surface

ACPD
12, 2783–2815, 2012

measurements and model estimations was found at both sites. The differences in measured and estimated GOM + PBM dry deposition at NY20 was largely explained by the differences in GOM concentrations (1.9 versus 1.2 $\mu g\,m^{-3}$ during the two different periods). Besides, the GOM concentrations at this site were very low and thus both concentration and dry deposition measurements were expected to have large errors (more discussion in Sect. 3.4). Surrogate surface measurements conducted at other locations in the USA also suggested similar range of GOM dry deposition (e.g., Lyman et al., 2007; Marsik et al., 2007).

The estimated dry deposition of GOM + PBM discussed above is substantially smaller than those simulated from Hg transport models (Zhang et al., 2012). It is believed that dry deposition estimated using AMNet data is more realistic than those estimated from Hg transport models because the surface-layer GOM and PBM concentrations simulated by the majority of the Hg transport models were higher by a factor of 2 to 10 compared to the recently available AMNet measured speciated concentrations in the Great Lakes region. Zhang et al. (2012) suggested that the emission inventory and the partitioning between GOM and PBM were the major reasons causing the large over-prediction of GOM and PBM concentrations. More recently, Kos et al. (2011) modified the GRAHM model after extensive sensitivity tests to improve the predicted surface-layer GOM and PBM concentrations. As a result, wet deposition prediction was also improved when compared to the MDN measurements. This further suggests that previously modeled Hg dry deposition of GOM + PBM were overestimated and were not as realistic as the values estimated using AMNet monitored speciated concentration data.

3.4 Sources of uncertainties

Potential uncertainties in estimated dry deposition can come from both uncertainties of measured concentrations and modeled V_d values. The instruments collecting speciated Hg concentration are subject to analytical artifacts which may cause measurement errors on the order of 10–40 % for all the Hg species (e.g., Gustin and Jaffe, 2010;

ACPD
12, 2783–2815, 2012

Lyman et al., 2010a, b; Huang et al., 2012). At the ELA, automated and manual calibrations were both performed and they agreed by an average of 4.9 % for GEM concentration (Cheng et al., 2011). At an urban site in Cleveland, Ohio, a recent study comparing the Tekran system and passive air samples found the relative percentage difference to be in the range of 4.0 to 44 % for GEM and 1.5 to 41 % for GOM during a several month experimental period (Huang et al., 2012). Apparently, large percentage errors were associated with low concentration cases. Different air sampler design can increase these differences (Lyman et al., 2010a). Considering that cases with highest concentrations dominate the annual dry deposition, the uncertainties in annual dry deposition estimation caused by uncertainties in measured concentrations should be lower than 40 %.

Uncertainties in calculated V_d are expected to be larger than in the measured concentrations. These uncertainties came from variation from model theory, errors in meteorological data used to drive the model, and the inaccurate representation of the surface characteristics. For example, many of the AMNet sites are located in areas of complex topography; the 15 km by 15 km average meteorological data may depart considerably from the specific meteorological conditions at an observation site.

If the dry deposition of GOM does behave like HNO_3, as frequently assumed in previous studies (Bullock et al., 2002; Miller et al., 2005; Marsik et al., 2007), then the uncertainties in GOM V_d should be generally within a factor of 2, as shown by a recent model intercomparison study (Flechard et al., 2011). No systematic error is identified in the estimated GOM dry deposition across all the sites. The relatively good agreement (e.g., within 30 % differences) between the estimates and the surrogate surface measurements at several sites discussed in Sect. 3.3 support this. However, an early study by Lyman et al. (2007), using a modified version of the present model, found the model underestimated GOM dry deposition by a factor of 2 or more compared with their surrogate surface measurements. They also stated that model results were sensitive to environmental and meteorological conditions, and application of the model to other land use categories or climatological conditions would likely yield different results.

ACPD
12, 2783–2815, 2012

Huang et al. (2012) using the same model as this study but with on-site meteorology, found the model only slightly underestimated their surrogate surface measurements. The same study also found the dry deposition measured using different surrogate surfaces differed by nearly a factor of 1.8. Thus, it is believed that uncertainties in modeled and measured dry deposition are in similar order of magnitude and are mostly within a factor of 2.

The PBM dry deposition fluxes presented in this study are likely conservative estimates since the ambient data collected by Tekran instrument excluded coarse particle Hg. As shown in a recent study on trace metal dry deposition, coarse particles play important and sometimes dominate role in the dry deposition budget (Zhang et al., 2011). Assuming 30 % of total PBM is in coarse particles (Landis and Keeler, 2002), PBM dry deposition need to be adjusted by a factor of 2 or more depending on the actual particle size distribution. At coastal locations where coarse PBM can be as high as 50 % (Feddersen et al., 2012), the estimated dry deposition needs to be adjusted by a factor of 3 to 5. However, the uncertainties in the sum of GOM + PBM dry deposition are likely to be within a factor of 2 considering PBM only contributes a small fraction to the dry deposition of GOM + PBM (more discuss in Sect. 3.5).

Due to the limited knowledge of GEM dry deposition and its bi-directional exchange feature, uncertainties in the estimated GEM dry deposition are difficult to quantify and can be very large under certain circumstances. Further assessments using litterfall measurements are presented in Sect. 3.5. Dry deposition estimates presented in this study are believed to be conservative estimates for all three forms of Hg at the majority of the locations based on the parameters given for V_d calculations. However, it is possible that net GEM dry deposition at a few sites might be overestimated if the GEM emission is underestimated.

Despite the uncertainties in the estimated dry deposition of all species, the major conclusions presented above remain effective. For example, even doubling the estimated GOM + PBM deposition would not change the relative importance of GOM + PBM and net GEM dry deposition.

ACPD
12, 2783–2815, 2012

3.5 Comparison with litterfall measurements

Direct dry deposition measurements for GEM are limited and there are no data available at multiple locations or at regional scales to evaluate the estimated net GEM dry deposition. However, litterfall measurements can be used to qualitatively (and to some extent, quantitatively) assess and constrain the estimated GEM and total dry deposition. A few factors need to be considered. The estimated dry deposition considered all land types surrounding the sites, included deposition to all media (leaves, tree branches, soils), and covered the whole year period; in contrast, litterfall deposition was only for forests, only considered deposition to leaves, and only covered seasons with leaves for deciduous forests (for conifers forest at the ELA, year-round litterfall and throughfall measurements were made). Additionally, the modeled dry deposition represented net dry deposition above the canopy; in contrast, litterfall deposition included Hg deposition from above the canopy as well as the interception of soil emitted Hg.

At all AMNet sites and the ELA site, estimated total dry deposition (GOM + PBM+net GEM) was in the range of 5.2 to 26 $\mu g\,m^{-2}\,yr^{-1}$ (except for NS01, 34.4 $\mu g\,m^{-2}\,yr^{-1}$), with GOM + PBM contributing only 0.4 to 8.1 $\mu g\,m^{-2}\,yr^{-1}$ to this total (Fig. 3). Litterfall deposition was in the range of 4 to 19 $\mu g\,m^{-2}\,yr^{-1}$ from all the sites (Risch et al., 2012a). In general, the model-estimated dry deposition was in the same range as the Hg measured in annual litterfall in Eastern and Central USA.

For the 6 sites (MD08, MD99, OH02, VT99, WV99, ELA) with both litterfall measurements and dry deposition estimates (Table 2), estimated total dry deposition was in the range of 11 to 16 $\mu g\,m^{-2}\,yr^{-1}$ and measured litterfall Hg were in the range of 9 to 19 $\mu g\,m^{-2}\,yr^{-1}$. At two forest-dominated sites (VT99 and WV99), estimated total dry deposition was not significantly different (e.g., 10–20 % difference) from the measured litterfall Hg and estimated net GEM dry deposition explains > 80 % of litterfall Hg. At another three sites (MD08, MD99 and OH02), net GEM dry deposition explains 45–60 % of the litterfall deposition while total dry deposition explained ~ 70–100 % of the litterfall deposition. There are several possibilities causing these discrepancies: (1) dry

ACPD
12, 2783–2815, 2012

deposition of GOM + PBM and the net GEM were underestimated due to various reasons including the overestimation of GEM reemission; (2) if only using forest canopy for estimating dry deposition at these three sites (nearly 50 % of the areas was not forest at these three sites as shown in Table S1), net GEM dry deposition would be higher and closer to the litterfall deposition (V_d is higher over forests than to any other surfaces); (3) it is also noted that the modeled re-emissions of GEM at these three sites were among the highest (MD08, OH02, MD99 in Fig. 2b); thus, part of the litterfall deposition might be from the interception of reemitted GEM from the soil, but not reflected in the modeled net GEM dry deposition.

Among the six co-located sites, ELA is the only site having net GEM dry deposition higher (by a factor of 1.8) than the litterfall deposition, which should be the case for locations with low soil Hg emissions. To better assess the estimated dry deposition at this site, long-term litterfall, throughfall, and open area wet deposition (Graydon et al., 2008, 2009) were used to construct the dry deposition budget. It is noticed that the litterfall value ($8.6\,\mu g\,m^{-2}\,yr^{-1}$; Fig. 3) was at the low end of previously published long-term estimates (8 to $12\,\mu g\,m^{-2}\,yr^{-1}$) that were probably more representative of the entire area. Also, the throughfall deposition (the difference between throughfall and open area wet deposition) was 0.15 to 0.85 times the litterfall deposition. Using median litterfall and net throughfall deposition, one can obtain an annual dry deposition estimation (as the total of litterfall and net throughfall, and ignore soil deposition/emission) of $\sim 15\,\mu g\,m^{-2}\,yr^{-1}$. This is in very good agreement with the model estimated dry deposition of $16.3\,\mu g\,m^{-2}\,yr^{-1}$ (Table 2).

The good agreement between estimated deposition and measured litterfall Hg suggests that the estimated dry deposition fluxes presented in this study are reasonable and conservative estimates. The speciated and total dry deposition numbers, in comparison with litterfall deposition numbers, suggest that litterfall deposition should be mostly from the assimilation of GEM, consistent with one previous study (Rea et al., 2002).

ACPD
12, 2783–2815, 2012

Dry deposition amounts presented in this study are best model estimates with large uncertainties. As mentioned in Sect. 3.4, GOM and PBM dry deposition are believed to be conservative estimates. To test the validity of the major conclusions generated above (e.g., the relative contribution of GEM and GOM + PBM, the sources of Hg in litetrfall), GOM and PBM dry deposition are adjusted by a factor of 2 and 4 (based on the potential uncertainties discussed in Sect. 3.4), respectively, which should represent their respective upper-end estimates. The increased GOM + PBM dry deposition for the six sites are listed in Table 2. With this adjustment, GEM dry deposition still dominated in the total dry deposition budget at four of the six sites; only at MD08 and WV99, GOM + PBM is equally important as GEM in the total dry deposition budget. Thus, the conclusions generated above remains effective regardless of the potential uncertainties in the estimated speciated dry deposition.

3.6 Relative contribution of dry and wet deposition

Annual wet deposition during 2007–2009 for the areas covering AMNet sites ranged from 6 to 9.0 $\mu g\,m^{-2}\,yr^{-1}$, and from 6 to 12 $\mu g\,m^{-2}\,yr^{-1}$ for the areas covering both AMNet and litterfall sites (Fig. 4). Comparing only GOM + PBM in the dry deposition budget, wet deposition plays a dominant role in the total (dry+wet) deposition budget at the majority of the sites. However, if net GEM dry deposition was included, dry deposition became dominant over or equivalent to the wet deposition at most locations studied here. The importance of dry deposition in the total deposition budget was also supported by the comparison of litterfall measurements with wet deposition measurements (Risch et al., 2012a). It is thus concluded that the dry and wet depositions are equally important on regional scales in Eastern North America, similar to the conclusions of Miller et al. (2005). But the relative contribution of dry and wet deposition to total deposition certainly depends on location, season and meteorological conditions.

ACPD
12, 2783–2815, 2012

4 Conclusions and recommendations

Despite the potential large uncertainties in concentration measurements and calculated deposition velocities, the estimated dry deposition of GOM + PBM agrees with limited surrogate surface dry deposition measurements and the estimated annual total dry deposition (GOM + PBM+net GEM) is in the same range as the annual litterfall Hg measurements. This provides some confidence on the estimated dry deposition. Results presented here suggest that GEM contributes much more than GOM + PBM to total dry deposition at the majority of sites studied here; the only exception is at locations close to significant point sources where GEM and GOM + PBM contribute equally to total dry deposition. This also implies that litterfall Hg is largely from the collection of GEM. Dry deposition has a similar range to wet deposition, and thus needs to be quantified as accurately as possible.

Future work should focus on estimating net GEM dry deposition more accurately, especially considering its dominant role as a contributor to total dry deposition. This will involve a better handling of the bi-directional exchange process, and a better understanding of GEM emission from natural surfaces. Recently, several research groups in the United States started measuring GEM gradients over forest canopies (10th ICMGP, Halifax, Canada, 23–29 July 2011). These measurements, together with modeling practices should improve our understanding of net GEM dry deposition. It is recommended, wherever possible, to collect data that can be used to quantify GEM fluxes both above the canopy and above the forest floor so that the data can be used to develop and improve bi-directional exchange models for GEM.

Supplementary material related to this article is available online at: http://www.atmos-chem-phys-discuss.net/12/2783/2012/acpd-12-2783-2012-supplement.pdf.

ACPD
12, 2783–2815, 2012

Acknowledgement. L. Zhang greatly appreciates I. Cheng for helpful discussion, A. Dastoor and A. Ryzhkov for providing GRAHM modeled GEM emission data, and AMNet site operators for their contribution in the collection of the speciated mercury ambient concentration data.

References

Amos, H. M., Jacob, D. J., Holmes, C. D., Fisher, J. A., Wang, Q., Yantosca, R. M., Corbitt, E. S., Galarneau, E., Rutter, A. P., Gustin, M. S., Steffen, A., Schauer, J. J., Graydon, J. A., Louis, V. L. St., Talbot, R. W., Edgerton, E. S., Zhang, Y., and Sunderland, E. M.: Gas-particle partitioning of atmospheric Hg(II) and its effect on global mercury deposition, Atmos. Chem. Phys., 12, 591–603, doi:10.5194/acp-12-591-2012, 2012.

Bash, J. O.: Description and initial simulation of a dynamic bidirectional air–surface exchange model for mercury in Community Multiscale Air Quality (CMAQ) model, J. Geophys. Res., 115, D06305, doi:10.1029/2009JD012834, 2010.

Bash, J. O., Bresnahan, P. A., and Miller, D. R.: Dynamic surface interface exchanges of mercury: A review and compartmentalized modeling framework. J. Appl. Meteorol. Climatol., 46, 1606–1618, 2007.

Brook, J. R., Zhang, L., Franco, D., and Padro J.: Description and evaluation of a model of deposition velocities for routine estimates of air pollutant dry deposition over North America. Part I. Model development, Atmos. Environ., 33, 5037–5052, 1999.

Bullock Jr., O. R. and Brehme, K. A.: Atmospheric mercury simulation using the CMAQ model: Formulation description and analysis of wet deposition results, Atmos. Environ., 36, 2135–2146, 2002.

Bullock, O. R., Atkinson, D., and Braverman, T.: The North American mercury model intercomparison study (NAMMIS): study description and model-to-model comparisons, J. Geophys. Res., 113, doi:10.1029/2008JD009803, 2008.

Castro, M. S., Moore, C., Sherwell, J., and Brooks, S. B.: Dry deposition of gaseous oxidized mercury in Western Maryland, Sci. Total Environ., doi:10.1016/j.scitotenv.2011.12.044, in press, 2012.

Cheng, I., Zhang, L., Blanchard, P., Graydon, J. A., and Louis, V. L. St.: Source-receptor relationships for speciated atmospheric mercury at the remote experimental lakes

ACPD

12, 2783–2815, 2012

area, Northwestern Ontario, Canada, Atmos. Chem. Phys. Discuss., 11, 31433–31474, doi:10.5194/acpd-11-31433-2011, 2011.
Dastoor, A. P. and Larocque, Y.: Global circulation of atmospheric mercury: a modeling study, Atmos. Environ., 38,147–161, 2004.
Dastoor, A. P., Davignon, D., Theys, N., Van Roozendael, M., Steffen, A., and Ariya, P. A.: Modeling dynamic exchange of gaseous elemental mercury at polar sunrise, Environ. Sci. Technol., 42, 5183–5188, 2008.
Feddersen, D., Talbot, R., Mao, H., Lombard, M., and Sive, B.: Aerosol size distribution of atmospheric mercury in marine and continental atmospheres, Atmos. Chem. Phys. Discuss., to be submitted, 2012.
Flechard, C. R., Nemitz, E., Smith, R. I., Fowler, D., Vermeulen, A. T., Bleeker, A., Erisman, J. W., Simpson, D., Zhang, L., Tang, Y. S., and Sutton, M. A.: Dry deposition of reactive nitrogen to European ecosystems: a comparison of inferential models across the NitroEurope network, Atmos. Chem. Phys., 11, 2703–2728, doi:10.5194/acp-11-2703-2011, 2011.
Engle, M. A., Tate, M. T., Krabbenhoft, D. P., Schauer, J. J., Kolker, A., Shanley, J. B., Bothner, M. H.: Comparison of atmospheric mercury speciation and deposition at nine sites across Central and Eastern North America, J. Geophys. Res.-Atmos., 115, D18306, doi:10.1029/2010JD014064, 2010.
Gbor, P. K., Wen, D., Meng, F., Yang, F., and Sloan, J. J.: Modeling of mercury emission, transport and deposition in North America, Atmos. Environ., 41, 1135–1149, 2007.
Graydon, J. A., St. Louis, V. L., Hintelmann, H., Lindberg, S. E., Sandilands, K. A., Rudd, J. W. M., Kelly, C. A., Hall, B. D., and Mowat, L. D.: Long-term wet and dry deposition of total and methyl mercury in the remote boreal ecoregion of Canada, Environ. Sci. Technol., 42, 8345–8351, 2008.
Graydon, J. A., St. Louis, V. L., Hintelmann, H., Lindberg, S. E., Sandilands, K. A., Rudd, J. W. M., Kelly, C. A., Tate, M. T., Krabbenhoft, D. P., and Lehnherr, I.: Investigation of uptake and retention of atmospheric Hg(II) by boreal forest plants using stable Hg isotopes, Environ. Sci. Technol., 43, 4960–4966, 2009.
Gustin, M. S. and Jaffe, D.: Reducing the uncertainty in measurement and understanding of mercury in the atmosphere, Environ. Sci. Technol., 44, 2222–2227, 2010.
Gustin, M. S., Lindberg, S. E., and Weisberg, P. J.: An update on the natural sources and sinks of atmospheric mercury, Appl. Geochem., 23, 482–493, 2008.
Huang, J., Choi, H.-D., Hopke, P. K., and Holsen, T. M.: Ambient mercury sources in Rochester,

ACPD
12, 2783–2815, 2012

NY: results from principle components analysis (PCA) of mercury monitoring network data, Environ. Sci. Technol., 44, 8441–8445, 2010.
Huang, J., Choi, H.-D., Landis, M. S., and Holsen, T. M.: An application of modified passive samplers for understanding of atmospheric mercury concentration and dry deposition spatial distribution, Atmos. Environ., submitted, 2012.
Keeler, G. J. and Dvonch, J. T.: Atmospheric mercury: A decade of observations in the Great Lakes, in: Dynamics of Mercury Pollution on Regional and Global Scales: Atmospheric Processes and Human Exposures around the World, edited by: Pirrone, N. and Mahaffey, K., Kluwer Ltd., Norwell, MA, 611–636, 2005.
Kos, G., Ryzhkov, A., and Dastoor, A.: Analysis of uncertainties in measurements and model for oxidised and particle-bound mercury, presented in the 10th International Conference on Mercury as a Global Pollutant, 24–29 July 2011, Halifax, Nova Scotia, Canada, abstract FS3-O11, 2011.
Landis, M. S. and Keeler, G., J.: Atmospheric mercury deposition to Lake Michigan during the Lake Michigan Mass Balance Study, Environ. Sci. Technol., 36, 4518–4524, 2002.
Landis, M. S., Stevens, R. K., Schaedlich, F., and Prestbo, E. M.: Development and characterization of an annular denuder methodology for the measurement of divalent inorganic reactive gaseous mercury in ambient air, Environ. Sci. Technol., 36, 3000–3009, 2002.
Lin, C. J., Pongprueksa, P., Lindberg, S. E., Pehkonen, S. O., Byun, D., and Jang, C.: Scientific uncertainties in atmospheric mercury models I: model science evaluation, Atmos. Environ., 40, 2911–2928, 2006.
Lin, C. J., Pongprueks, P., Bullock Jr., O. R., Lindberg, S. E., Pehkonen, S. O., Jang, C., Braverman, T., and Ho, T. C.: Scientific uncertainties in atmospheric mercury models II: sensitivity analysis in the conus domain, Atmos. Environ., 41, 6544–6560, 2007.
Lindberg, S., Bullock Jr., O. R., Ebinghaus, R., Engstrom, D., Feng, X., Fitzgerald, W., Pirrone, N., and Seigneur, C.: A synthesis of progress and uncertainties in attributing the sources of mercury in deposition, Ambio, 36, 19–32, 2007.
Lyman, S. N., Gustin, M. S., Prestbo, E. M., and Marsik, F. J.: Estimation of dry deposition of atmospheric mercury in Nevada by direct and indirect methods, Environ. Sci. Technol., 41, 1970–1976, 2007.
Lyman, S. N., Gustin, M. S., and Prestbo, E. M.: A passive sampler for ambient gaseous oxidized 424 mercury concentrations, Atmos. Environ., 44, 246–252, 2010a.
Lyman, S. N., Jaffe, D. A., and Gustin, M. S.: Release of mercury halides from KCl denuders

ACPD
12, 2783–2815, 2012

in the presence of ozone, Atmos. Chem. Phys., 10, 8197–8204, doi:10.5194/acp-10-8197-2010, 2010b.
Mao, H. and Talbot, R.: Speciated mercury at marine, coastal, and inland sites in New England – Part 1: Temporal variability, Atmos. Chem. Phys. Discuss., 11, 32301–32336, doi:10.5194/acpd-11-32301-2011, 2011.
Marsik, F. J., Keeler, G. J., and Landis, M. S.: The dry deposition of speciated mercury to the Florida Everglades: measurements and modeling, Atmos. Environ., 41, 136–149, 2007.
Mason, R. P. and Sheu, G.-R.: The role of the ocean in the global mercury cycle, Global Biogeochem. Cy., 16, 1093, 2002.
Mason, R. P., Abbott, M. L., Bodaly, R. A., Bullock Jr., O. R., Driscoll, C. T., Evers, D., Lindberg, S. E., Murray, M., and Swain, E. B.: Monitoring the response to changing mercury deposition, Environ. Sci. Technol., 39, 14A–22A, 2005.
Miller, E. K., Vanarsdale, A., Keeler, G. J., Chalmers, A., Poissant, L., Kamman, N. C., and Brulotte, R.: Estimation and mapping of wet and dry mercury deposition across Northeastern North America, Ecotoxicology, 14, 53–70, 2005.
National Atmospheric Deposition Program (NADP): AMNet Standard Operating Procedure Site Report A: Each Visit/Weekly Maintenance. Illinois State Water Survey, Champaign IL, available at: http://nadp.isws.illinois.edu/amn/docs/, last access: 20 November 2011a.
National Atmospheric Deposition Program (NADP): AMNet Standard Operating Procedure Site Report B: Glassware Change-out/Monthly Maintenance, Illinois State Water Survey, Champaign IL, available at: http://nadp.isws.illinois.edu/amn/docs/, last access: 20 November 2011b.
National Atmospheric Deposition Program (NADP): AMNet Standard Operating Procedure Site Report C: Quarterly Maintenance, Illinois State Water Survey, Champaign IL, available at: http://nadp.isws.illinois.edu/amn/docs/, last access: 20 November 2011c.
National Atmospheric Deposition Program (NADP): AMNet Standard Operating Procedure Site Report D: Annual/As Needed Maintenance, Illinois State Water Survey, Champaign IL, available at: http://nadp.isws.illinois.edu/amn/docs/, last access: 20 November 2011d.
National Atmospheric Deposition Program (NADP): Atmospheric Mercury Network Data Management Manual, Version 1.4, Illinois State Water Survey, Champaign IL, available at: http://nadp.isws.illinois.edu/amn/docs/, last access: 20 November 2011e.
Pongprueksa, P., Lin, C. J., Lindberg, S. E., Jang, C., Braverman, T., Bullock Jr., O. R., Ho, T. C., and Chu, H. W.: Scientific uncertainties in atmospheric mercury models III: boundary and

ACPD
12, 2783–2815, 2012

initial conditions, model grid resolution, and Hg(II) reduction mechanism, Atmos. Environ., 42, 1828–1845, 2008.
Prestbo, E. M. and Gay, D. A.: Wet deposition of mercury in the US and Canada, 1996–2005: results and analysis of the NADP mercury deposition network (MDN), Atmos. Environ., 43, 4223–4233, 2009.
Rea, A. W., Lindberg, S. E., Scherbatskoy, T., and Keeler, G. J.: Mercury accumulation in foliage over time in two northern mixed hardwood forests, Water Air Soil Pollut., 133, 49–67, 2002.
Risch, M. R., DeWild, J. F., Krabbenhoft, D. P., Kolka, R. K., Zhang, L.: Mercury in litterfall at selected national atmospheric deposition program mercury deposition network sites in the Eastern United States, 2007–2009. Environ. Pollut., 161, 284–290, 2012a
Risch, M. R., Gay, D., Fowler, K., Keeler, G., Blanchard, P., Backus, S., Barres, J., and Dvonch, T.,: Spatial patterns and statistical trends in mercury concentrations, precipitation, and mercury wet deposition in the North American Great Lakes region, 2002–2008, Environ. Pollut., 161, 261–271, 2012b.
Sakata, M. and Asakura, K.: Evaluating relative contribution of atmospheric mercury species to mercury dry deposition in Japan, Water Air Soil Pollut., 193, 51–63, 2008.
Schroeder, W. H., Munthe, J., and Lindqvist, O.: Cycling of mercury between water, air, and soil compartments of the environment, Water Air Soil Pollut. 48, 337–347, 1989.
Selin, N. E., Jacob, D. J., Park, R. J., Yantosca, R. M., Strode, S., Jaegle, L., and Jaffe, D.: Chemical cycling and deposition of atmospheric mercury: global constraints from observations, J. Geophys. Res., 112, D02308, doi:10.1029/2006JD007450, 2007.
Sprovieri, F., Pirrone, N., Ebinghaus, R., Kock, H., and Dommergue, A.: A review of worldwide atmospheric mercury measurements, Atmos. Chem. Phys., 10, 8245–8265, doi:10.5194/acp-10-8245-2010, 2010.
Vanarsdale, A., Weiss, J., Keeler, G., Miller, E., Boulet, G., Brulotte, R., and Poissant, L.: Patterns of mercury deposition and concentration in Northeastern North America (1996–2002), Ecotoxicology, 14, 37–52, 2005.
Xu, X., Yang, X., Miller, D. R., Helble, J. J., and Carley, R. J.: Formulation of bi-directional atmosphere-surface exchanges of elemental mercury, Atmos. Environ., 33, 4345–4355, 1999.
Zhang, L., Gong, S., Padro, J., and Barrie, L. A.: A size-segregated particle dry deposition scheme for an atmospheric aerosol module, Atmos. Environ., 35, 549–560, 2001.
Zhang, L., Brook, J. R., and Vet, R.: A revised parameterization for gaseous dry deposition

ACPD
12, 2783–2815, 2012

in air-quality models, Atmos. Chem. Phys., 3, 2067–2082, doi:10.5194/acp-3-2067-2003, 2003.

Zhang, L., Wright, L. P., and Blanchard, P.: A review of current knowledge concerning dry deposition of atmospheric mercury, Atmos. Environ., 43, 5853–5864, 2009.

Zhang, L., Fang, G. C., Liu, C. K., Huang, Y. L., Huang, J. H., and Huang, C. S.: Dry deposition fluxes and deposition velocities of seven trace metal species at five sites in Central Taiwan – a summary of surrogate surface measurements and a comparison with model estimation, Atmos. Chem. Phys. Discuss., 11, 32847–32875, doi:10.5194/acpd-11-32847-2011, 2011.

Zhang, L., Blanchard, P., Johnson, D., Dastoor, A., Ryzhkov, A., Lin, C.-J., Vijayaraghavan, K., Gay, D., Holsen, T. M., Huang, J., Graydon, J. A., St. Louis, V. L., Castro, M. S., Miller, E. K., Marsik, F., Lu, J., Poissant, L., Pilote, M., and Zhang, K. M.: Assessment of modeled mercury deposition over the Great Lakes region, Environ. Pollut., 161, 272–283, 2012.

ACPD

12, 2783–2815, 2012

Table 1. List of AMNet site information.

AMNet Site ID	Site name	Lat and lon	Data coverage	Dominant land type within 1 km circle	Site category
MD08	Piney Reservoir	39.7053, −79.0122	Jan/08–Dec/09	Grass, mixed forest, shrubs, lake	Rural
MD99	Beltsville	39.0284, −76.8171	Jan–Feb/08, May–Jun/08, Apr–Sep/09, Dec/09	Forest, urban	Suburban
MS12	Grand Bay NERR	30.4294, −88.4277	Jan/08–Dec/09 except Sep/08	Woody wetland, shrubs, forest	Rural
NH06	Thompson Farm	43.1100, −70.9500	Feb/09–Dec/09	Mixed forest, crops	Rural
NJ05	Brigantine	39.4020, −74.3790	Jul–Aug/09, Oct–Dec/09	Wetland, lake, forest	Suburban
NJ30	New Brunswick	40.4728, −74.4226	May–Jun/09, Sep–Oct/09	Urban, crop, forest, wetland	Urban
NJ32	Chester	40.7876, −74.6763	May–Aug/08, Oct–Dec/08, Jan/09, Apr–Sep/09	Urban, forest, wetland	Suburban
NJ54	Elizabeth Lab	40.6414, −74.2084	Jan–Feb/08, Sep–Oct/08, Apr–Jun/09	Urban	Urban
NS01	Kejimkujik National Park	44.4328, −65.2056	Jan–Dec/09	Forest	Rural
NY06	Bronx	40.8680, −73.8782	Aug/08–Dec/09	Urban	Urban
NY20	Huntington Wildlife	43.9731, −74.2231	Jan–Dec/08	Forest, lake, wetland	Rural
NY43	Rochester	43.1463, −77.5481	Jan/08–Jan/09	Urban	Suburban
NY95	Rochester_B	43.1463, −77.5481	Sep/08–Dec/09	Urban	Suburban
OH02	Athens Super Site	39.3078, −82.1182	Feb/08–Dec/09	Forest, shrubs	Rural
OK99	Stilwell	35.7514, −94.6717	Jan/09–Dec/09	Grass, forest	Rural
UT96	Antelope Island	41.0467, −112.0248	Jul–Dec/09	Grass, crops	Suburban
UT97	Salt Lake City	40.7118, −111.9609	Dec/08–Dec/09	Urban	Urban
VT99	Underhill	44.5283, −72.8684	Jan/08–Dec/09	Forest, grass, lake	Rural
WV99	Canaan Valley Institute	39.0636, −79.4222	Nov–Dec/08, Feb–Mar/09	Forest	Rural
ELA	Experimental Lakes Area	49.664, −93.721	Jan/08, May–Jul/08, Sep/08–Dec/09	Forest	Rural

ACPD
12, 2783–2815, 2012

Table 2. Estimated speciated and total dry deposition ($\mu g\,m^{-2}\,yr^{-1}$) and measured litterfall deposition ($\mu g\,m^{-2}\,yr^{-1}$) at six sites. The last column represents upper-end estimation of GOM + PBM dry deposition by incorporating the potential uncertainties.

Site ID	GOM	PBM	GOM+ PBM	Net GEM	Total dry deposition	Litterfall	Increased GOM + PBM
MD08	7.8	0.30	8.1	6.8	14.9	15.3	16.8
MD99	1.3	0.32	1.6	9.0	10.6	15.5	3.9
OH02	3.0	0.38	3.4	9.9	13.3	18.8	7.5
VT99	0.72	0.41	1.1	11.7	12.8	11.3	3.1
WV99	3.6	0.44	4.0	8.2	12.2	9.9	9.0
ELA	0.49	0.25	0.74	15.6	16.3	8.6	2.0

ACPD
12, 2783–2815, 2012

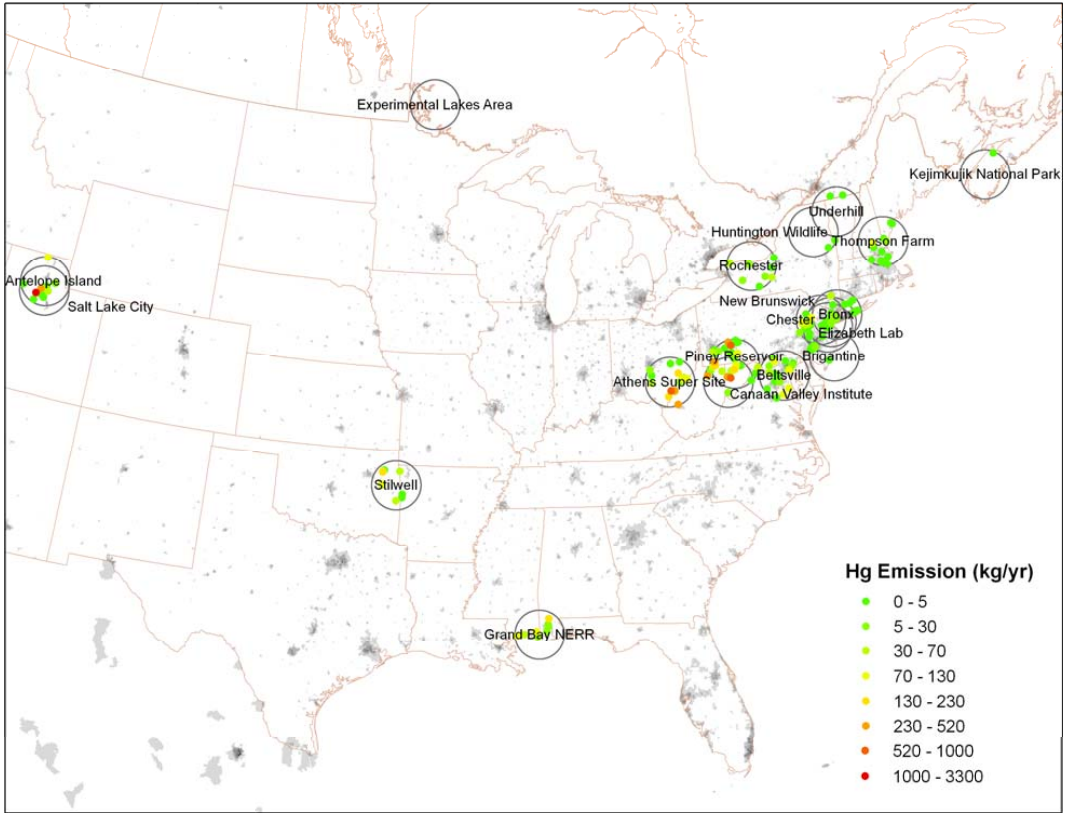

Fig. 1. Locations of the AMNet sites where Hg dry deposition were estimated. Also shown are Hg point source emissions with a 100 km circle of each site.

ACPD
12, 2783–2815, 2012

Estimation of speciated and total mercury dry deposition

L. Zhang et al.

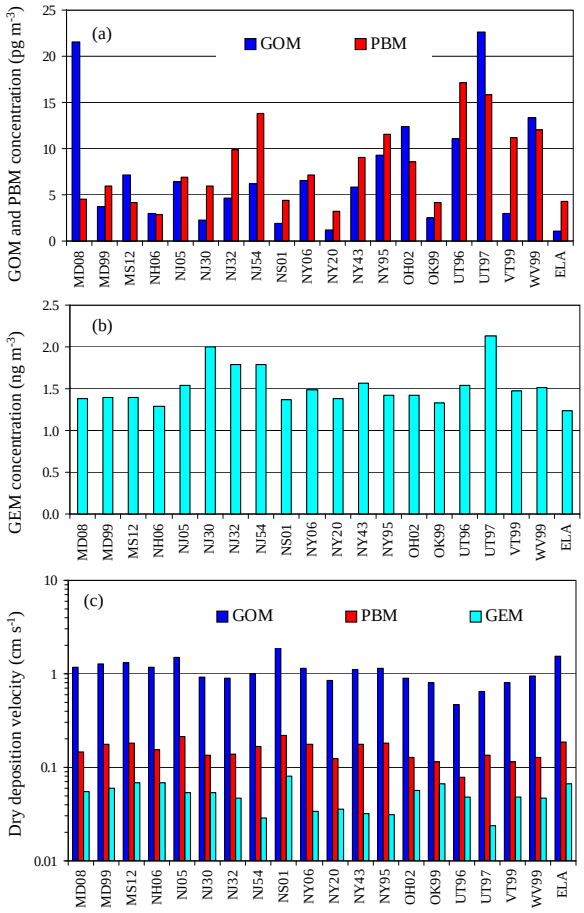

Fig. 2. Annual average concentrations for GOM, PBM (pg m^{-3}) and GEM (ng m^{-3}) and annual dry deposition velocity (V_d in cm s^{-1}).

ACPD
12, 2783–2815, 2012

Estimation of speciated and total mercury dry deposition

L. Zhang et al.

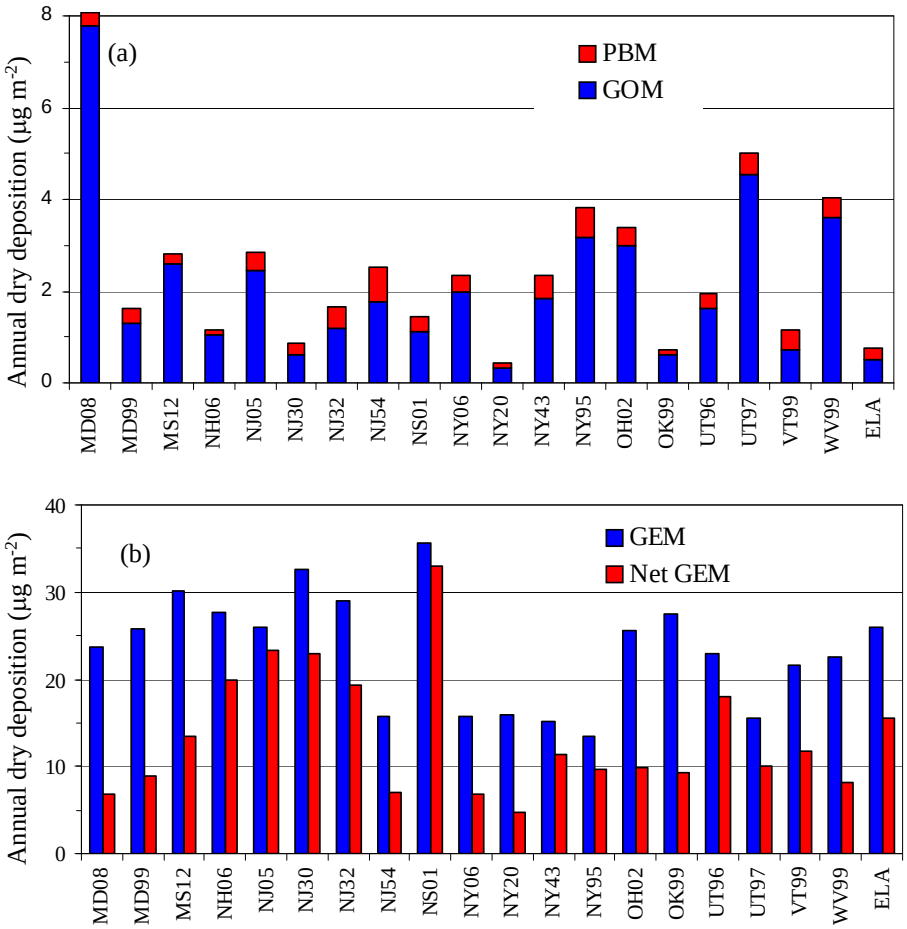

Fig. 3. Annual average speciated dry deposition fluxes (μg m^{-2}). Net GEM flux is the GEM dry flux minus GRAHM modeled annual GEM reemission and natural emission fluxes.

ACPD
12, 2783–2815, 2012

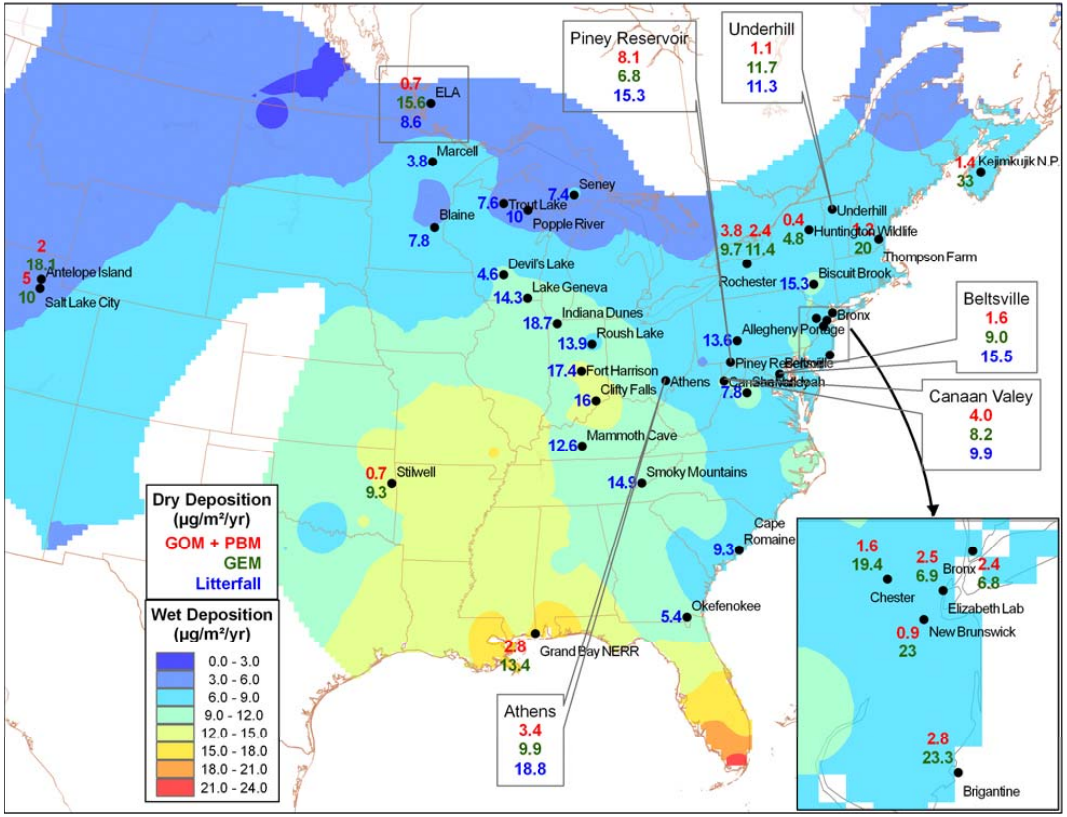

Fig. 4. Comparisons of estimated dry deposition of GOM + PBM and GEM from 2008 and 2009 speciated concentrations with litterfall deposition collected during 2007–2009 and with wet deposition monitored during 2007–2009.

ACPD
12, 2783–2815, 2012